AD-A150 926 RESPONSE OF SATURATED SOILS TO DYNAMIC LOADING(U) OHIO 1/1
STATE UNIV RESEARCH FOUNDATION COLUMBUS
R S SANDHU ET AL. JUN 84 OSURF-715107-84-4
UNCLASSIFIED AFOSR-TR-85-0092 AFOSR-83-0055 F/G 8/13 NL

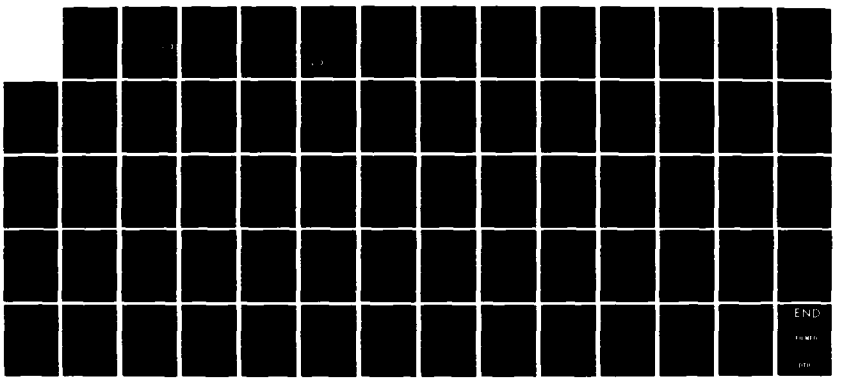

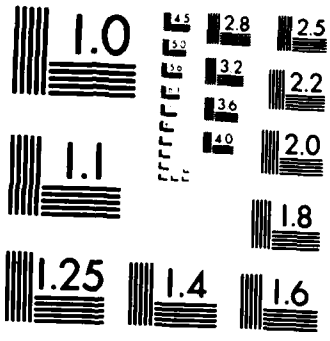

(2)

RF Project 763420/715107
Annual Report

RESPONSE OF SATURATED SOILS TO DYNAMIC LOADING

Ranbir S. Sandhu, S. J. Hong and Baher L. Aboustit
Department of Civil Engineering

DEPARTMENT OF THE AIR FORCE
Air Force Office of Scientific Research
Bolling Air Force Base, D.C. 20332

Grant No. AFOSR-83-0055

June, 1984

OSU
The Ohio State University
Research Foundation
1314 Kinnear Road
Columbus, Ohio 43212

Unclassified

SECURITY CLASSIFICATION OF THIS PAGE

REPORT DOCUMENTATION PAGE

1a. REPORT SECURITY CLASSIFICATION: Unclassified	1b. RESTRICTIVE MARKINGS
2a. SECURITY CLASSIFICATION AUTHORITY	3. DISTRIBUTION/AVAILABILITY OF REPORT: Approved for Public Release Distribution Unlimited.
2b. DECLASSIFICATION/DOWNGRADING SCHEDULE	
4. PERFORMING ORGANIZATION REPORT NUMBER(S): OSURF-715107-84-4	5. MONITORING ORGANIZATION REPORT NUMBER(S): AFOSR-TR- 85-0092
6a. NAME OF PERFORMING ORGANIZATION: The Ohio State Research Foundation; 6b. OFFICE SYMBOL (If applicable)	7a. NAME OF MONITORING ORGANIZATION: Same as #8
6c. ADDRESS (City, State and ZIP Code): Department of Civil Engineering, 1314 Kinnear Road, Columbus, OH 43212	7b. ADDRESS (City, State and ZIP Code)
8a. NAME OF FUNDING/SPONSORING ORGANIZATION: Air Force Office of Scientific Research; 8b. OFFICE SYMBOL (If applicable): AFOSR/NA	9. PROCUREMENT INSTRUMENT IDENTIFICATION NUMBER: AFOSR-83-0055
8c. ADDRESS (City, State and ZIP Code): Bolling AFB, DC 20332-6448	10. SOURCE OF FUNDING NOS.

PROGRAM ELEMENT NO	PROJECT NO.	TASK NO.	WORK UNIT NO
61102F	2307	C1	

11. TITLE (Include Security Classification): Response of Saturated Soils to Dynamic Loading (Unclassified)

12. PERSONAL AUTHOR(S): Ranbir S. Sandhu Soon J. Hong Baher L. Aboustit

13a. TYPE OF REPORT	13b. TIME COVERED	14. DATE OF REPORT (Yr., Mo., Day)	15. PAGE COUNT
Annual	FROM 1 Feb 83 TO 31 Jan 84	June, 1984	65

16. SUPPLEMENTARY NOTATION

17 COSATI CODES			18. SUBJECT TERMS (Continue on reverse if necessary and identify by block number)
FIELD	GROUP	SUB GR	Finite Element Methods Dynamics of Saturated Soils Wave Propagation

19. ABSTRACT (Continue on reverse if necessary and identify by block number)

The transient response of saturated porous soils to time dependent boundary conditions is analyzed. Galerkin finite element method is used to set up the spatial discretization of Biot's equations of wave propagation through linearly elastic fluid-saturated porous medium. Wilson's θ-γ-θ algorithm is used to integrate the equations of motion. The procedure is applied to several one-dimensional steady state and transient problems. Excellent agreement with the analytic solutions was obtained with 'proper' selection of time-integration parameters.

20. DISTRIBUTION/AVAILABILITY OF ABSTRACT	21. ABSTRACT SECURITY CLASSIFICATION
UNCLASSIFIED/UNLIMITED ☒ SAME AS RPT ☐ OTIC USERS ☐	Unclassified

22a. NAME OF RESPONSIBLE INDIVIDUAL	22b. TELEPHONE NUMBER (Include Area Code)	22c. OFFICE SYMBOL
Lt. Col. Lawrence D. Hokanson	202/767-4935	AFOSR/NA

DD FORM 1473, 83 APR EDITION OF 1 JAN 73 IS OBSOLETE

SECURITY CLASSIFICATION OF THIS PAGE

OSURF-715107-84-4

RESPONSE OF SATURATED SOILS TO DYNAMIC LOADING

By

Ranbir S. Sandhu
S.J. Hong
Baher L. Aboustit

Department of Civil Engineering

June 1984

AIR FORCE OFFICE OF SCIENTIFIC RESEARCH
Grant: AFOSR-83-0055

Geotechnical Engineering Report No.13

The Ohio State University Research Foundation
1314 Kinnear Road, Columbus, Ohio 43212

FOREWORD

The investigation reported herein is part of the research project at The Ohio State University, Columbus, Ohio supported by the Air Force Office of Scientific Research Grant 83-0055. Lt. Col. John J. Allen was the Program Manager at the commencement of the project. Lt. Col. Lawrence D. Hokanson was the Program Manager from July 1, 1983 onwards. The research project was started Feburary 1, 1983 and is continuing. The present report documents part of the work done up to January 31, 1984. At The Ohio State University, the project is supervised by Dr. Ranbir S. Sandhu, Professor, Department of Civil Engineering. The computer program modification were carried out by Dr. Baher L. Aboustit, Post-doctoral Reseach Associate. The analyses reported herein were started by Dr. Aboustit and completed by Mr. Soon-jo Hong, graduate student, who also prepared the documentation on the Ohio State University Computer System. The Instruction and Research Computer Center at The Ohio State University provided the computational facilities.

ABSTRACT

The transient response of saturated porous soils to time dependent boundary conditions is analyzed. Galerkin finite element method is used to set up the spatial discretization of Biot's equations of wave propagation through linearly elastic fluid-saturated porous medium. Wilson's β-γ-θ algorithm is used to integrate the equations of motion. The procedure is applied to several one-dimensional steady state and transient problems. Excellent agreement with the analytic solution was obtained with 'proper' selection of time-integration parameters. There is apparent need for developing reliable time-integration procedures.

TABLE OF CONTENTS

LIST OF FIGURES

LIST OF TABLES

SECTION I

INTRODUCTION

Biot (2,3) developed the field equations for propagations of waves through fluid-saturated elastic porous media. Lagrange equation of motion was set up assuming the existence of a dissipation function in terms of the relative velocity of the two constituents. By assuming the existence of a strain energy density function for the mixture, the equations of motion were written in terms of the displacements of the solid and the fluid. Hsieh and Yew (13) combined the theory of mixtures and Biot's assumption that the fluid acts over the pore space, to provide similar equations to Biot's equation (3) but with variable porosity. Garg (10) extended the theory to elastic-plastic soils. Ishihara (15) examined Biot's work in terms of physical constants which are related to the compressibilities of individual constituent materials. Prevost (17) assumed Newtonian fluid behavior and the soil to be elasto-plastic.

Most analytical solutions for the initial boundary value problem of wave propagation through saturated porous media provide only the harmonic component of the solution. Deresiewicz (6,7) obtained solution for the reflection of plane waves (2) and Love waves at a free plane. Zienkiewicz et al.(24) obtained the solution for a half space subjected to harmonic tractions. Garg et al.(11) presented the exact transient as well as the steady state solutions for compressional wave propagation through a porous elastic solid and developed finite difference proce-

dures for numerical solution. Chakroborty and Dey (4) obtained the solution for Love waves in saturated media underlain by heterogeneous elastic media.

Although the finite element method has been extensively used for analysis of quasi-static consolidation problems, e.g. Sandhu (21), its application to the dynamic response of saturated soils is still in its infancy. Ghaboussi and Wilson (12) used Sandhu and Pister's (19) approach to construct a variational principle, of the Gurtin type, equivalent to Biot's (3) field equations including initial as well as boundary conditions. This variational principle was the basis for a finite element discretization, in which the Gurtin type approach was replaced by the β- γ - θ method for the time-domain integration. In the spatial discretization, a one-dimensional element was used with nodal values of the solid displacement and the relative displacement of the fluid as generalized coordinates. The problem of a soil layer subjected to unit step loading was analyzed. The problem was solved by two methods based on lumped mass and on consistent mass, respectively. Waves appeared to propagate faster when consistent mass formulation was used. This was ascribed to inertial coupling in this formulation. Ghaboussi and Wilson (12) did not present any comparison with exact solution. Garg (11) considered this unsatisfactory as the results from the two approaches differed considerably. Prevost (17) used the Galerkin approach for spatial discretization and Hughes' (14) implicit-explicit algorithm for time domain integration. Bilinear four noded isoparametric elements were used with nodal point values of displacement of the solid and the fluid as the unknown parameters. Assumption of Newtonian fluid behavior lead to

nonsymmetric damping matrices. Two-dimensional analysis was actually used to solve a one-dimensional problem with finite length. For relatively large permeability, Prevost compared his results with the exact solution for a solid with no pores. This was incorrect because non-porous solid represents a strong coupling, while a material with high permeability is weakly coupled (11).

The purpose of this investigation was to develop an effective finite element computer program based on the Biot's theory and evaluate it against available analytical solutions. A Galerkin approach was used to set up the semi-discrete matrices spatially and the β-γ-θ algorithm is used for the time domain integration. Nodal values of the solid displacement and relative displacement of the fluid with respect to the solid skeleton are used as the unknown quantities. A computer program was written to handle one-dimensional as well as plane-strain problems. One-dimensional linear element and four node and eight node isoparametric two-dimensional elements were used. The development is essentially similar to Ghaboussi and Wilson's (12). The program was applied to numerical solution of several one-dimensional problems for quasi-static as well as dynamic problems for which exact solutions are available. The results showed excellent agreement between the approximate and the exact solution.

SECTION II summarizes the governing field equations following Biot (3). The finite element development is given in section III. SECTION IV describes the example problems. Results of the numerical solution procedures are evaluated in SECTION V.

SECTION II

FIELD EQUATIONS GOVERNING DYNAMICS OF FLUID-SATURATED ELASTIC SOILS

Biot's (3) equations of motion for an elastic porous medium saturated with a compressible fluid may be written in standard indicial notation as;

$$[E_{ijkl}u_{k,l} + \alpha M(\alpha u_{k,k} + w_{k,k})\delta_{ij}]_{,j} + \rho f_i = \rho\ddot{u}_i + \frac{1}{f}\rho_2\ddot{w}_i \qquad (1)$$

$$[M(\alpha u_{k,k} + w_{k,k})]_{,i} + \frac{1}{f}\rho_2 f_i = \frac{1}{f}\rho_2\ddot{u}_i + \frac{1}{f^2}\rho_2\ddot{w}_i + \frac{1}{K}\dot{w}_i \qquad (2)$$

where u_i, w_i, f_i, E_{ijkl} denote the cartesian components, respectively, of the solid displacement vector, the relative fluid displacement vector, the body force vector per unit mass and the isothermal elasticity tensor. ρ is mass density of the saturated soil and ρ_2 that of water per unit bulk volume. f, K, α, M are, respectively, the porosity, the permeability, the solid compressibility and the fluid compressibility. The superposed dot implies a time derivative. All the functions are defined over the cartesian product R x $[0,\infty)$ where R is the spatial region of interest and $[0,\infty)$ is the positive interval of time. With these field equations, we associate the following boundary conditions.

$$u_i(t) = u_i(t) \quad \text{on } S_{1i} \qquad (3)$$

$$t_i = \tau_{ij} n_j = (E_{ijkl} u_{k,l} + \alpha \pi \delta_{ij}) n_j = \hat{t}_i \quad \text{on } S_{2i} \tag{4}$$

$$\pi(t) = M(\alpha u_{k,k} + w_{k,k}) = \hat{\pi}(t) \quad \text{on } S_3 \tag{5}$$

$$w_i(t) = \hat{w}_i(t) \quad \text{on } S_4 \tag{6}$$

where S_{1i}, S_{2i} are complementary subsets of the boundary S of the spatial region of interest and so are S_3, S_4. The initial conditions for the problem are given by:

$$u(\underline{x}, 0) = u_o(x)$$

$$\dot{u}(\underline{x}, 0) = \dot{u}_o(x)$$

$$w(\underline{x}, 0) = w_o(x)$$

$$\dot{w}(\underline{x}, 0) = \dot{w}_o(x)$$

SECTION III

FINITE ELEMENT FORMULATION

3.1 SPATIAL DISCRETIZATION

Spatial discretization, APPENDIX A, of the governing equations for the two-field formulation leads to the following matrix equations;

$$\begin{bmatrix} K_{ss} & K_{sf} \\ K_{sf}^T & K_{ff} \end{bmatrix} \begin{Bmatrix} u \\ w \end{Bmatrix} + \begin{bmatrix} 0 & 0 \\ 0 & C_{ff} \end{bmatrix} \begin{Bmatrix} \dot{u} \\ \dot{w} \end{Bmatrix} + \begin{bmatrix} M_{ss} & M_{sf} \\ M_{sf}^T & M_{ff} \end{bmatrix} \begin{Bmatrix} \ddot{u} \\ \ddot{w} \end{Bmatrix} = \begin{Bmatrix} R_s \\ R_f \end{Bmatrix} \quad (7)$$

The development of these vectors and matrices is given in Appendix A. These equations assume no inherent damping in the system as a whole. The only damping component is associated with relative motion.

Ghaboussi and Wilson (12) introduced damping as a linear combination of the stiffness and the mass matrix in the following form;

$$C_{ss} = a_1(M_{ss} - f^2 M_{ff}) + a_2(K_{ss} - \alpha^2 K_{ff}) \quad (8)$$

where a_1, a_2 are constants and f, α have been defined in SECTION II. The structural damping matrix is a linear combination of the mass and the effective stiffness of the soil. Comparing with Equation (1), $(K_{ss}-\alpha^2 K_{ff})u$ corresponds to $(E_{ijkl}u_{k,l})_{,j}$. The quantity M_{ss} corresponds to ρ in Equation (1) and M_{ff} to ρ_2/f^2 in Equation (2). Hence, $M_{ss}-f^2M_{ff}$ corresponds to ρ_1.

3.2 TIME DOMAIN INTEGRATION

The discretized equations of motion, Equation (7) can be rewritten as

$$M\ddot{U} + C\dot{U} + KU = R \tag{9}$$

in which

$$U = \begin{Bmatrix} u \\ \\ w \end{Bmatrix} \qquad M = \begin{bmatrix} M_{ss} & M_{sf} \\ \\ M_{sf}^{T} & M_{ff} \end{bmatrix} \qquad C = \begin{bmatrix} C_{ss} & 0 \\ \\ 0 & C_{ff} \end{bmatrix}$$

$$K = \begin{bmatrix} K_{ss} & K_{sf} \\ \\ K_{sf}^{T} & K_{ff} \end{bmatrix} \qquad R = \begin{Bmatrix} R_s \\ \\ R_f \end{Bmatrix} \tag{10}$$

Wilson's β - γ - θ algorithm was used to integrate the equations of motion. In summary, the algorithm works as follows.

The displacements and velocities at time $t_n + \theta\,\Delta t$ can be expressed in terms of U, $\dot{U}$, $\ddot{U}$ at time t_n as

$$U_{n+\theta} = U_n + \theta\Delta t\dot{U}_n + (1/2-\beta)\,\theta^2(\Delta t)^2\,\ddot{U}_n + \beta\theta^2(\Delta t)^2\,\ddot{U}_{n+1} \tag{11}$$

$$\dot{U}_{n+\theta} = \dot{U}_n + (1-\gamma)\,\theta\Delta t\ddot{U}_n + \gamma\theta\Delta t\ddot{U}_{n+1} \tag{12}$$

in which β and γ are Newmark's coefficients (16).

Substitution of Equations (11) and (12) into Equation (9) yields

$$K^* U_{n+\theta} = R^*_{n+\theta} \tag{13}$$

in which

$$K^* = K + \frac{1}{\beta\theta^2(\Delta t)^2} M + \frac{\gamma}{\beta\theta\Delta t} C$$

$$R^*_{n+\theta} = R_{n+\theta} + \frac{1}{\beta\theta^2(\Delta t)^2} Ma_{n+\theta} + \frac{\gamma}{\beta\theta\,\Delta t} Cb_{n+\theta} \tag{14}$$

$$a_{n+\theta} = U_n + \theta\,\Delta t\dot{U}_n + (1/2-\beta)\,\theta^2(\Delta t)^2\,\ddot{U}_n$$

$$b_{n+\theta} = U_n + (1-\beta/\gamma)\theta\,\Delta t\dot{U}_n + (1/2-\beta/\gamma)\theta^2(\Delta t)^2\,\ddot{U}_n$$

Assuming cubic expansion of nodal point displacement over a time interval in terms of displacement, velocity and acceleration at time t_n, the displacement, velocity and acceleration at time $t_n + \Delta t$ can be expressed as

$$U_{n+1} = \frac{1}{\theta^3} U_{n+\theta} + (1 - \frac{1}{\theta^3})U_n + (1 - \frac{1}{\theta^2})\,\Delta t\dot{U}_n + 1/2(1 - \frac{1}{\theta})(\Delta t)^2\,\ddot{U}_n$$

$$\dot{U}_{n+1} = \frac{\gamma}{\beta\theta^3(\Delta t)^2}(U_{n+\theta} - U_n) + (1 - \frac{\gamma}{\beta\theta^2})\dot{U}_n + (1 - \frac{\gamma}{2\beta\theta})\,t\ddot{U}_n \tag{15}$$

$$\ddot{U}_{n+1} = \frac{1}{\theta^3(\Delta t)^2}(U_{n+\theta} - U_n) - \frac{1}{\beta\theta^2\Delta t}\dot{U}_n + (1 + \frac{1}{2\beta\theta})\,\ddot{U}_n$$

Various values for b and 0 can lead to various integration schemes (12). For $\theta = 1$, the stability of the β- γ method has been examined. Zienkiewicz (23) gives the following criteria for the undamped response of a linear system.

$$\gamma > 1/2$$

$$\beta > 1/4(1/2 + \gamma)^2 \qquad (16)$$

$$1/2 + \beta + \gamma \geq 0$$

SECTION IV

EXAMPLE PROBLEMS

4.1 INTRODUCTION

Several examples with known analytical solution were solved to check the validity of the method and the correctness of code. These examples included

a. Quasi-static soil consolidation

b. Dynamic response of an elastic layer of single material

c. Response of a fluid-saturated soil layer

All the problems deal with compressional wave propagation in an initially undisturbed, homogeneous, isotropic, elastic, porous or non-porous system to dynamic loading. The system for c above was subjected to spatially uniform surface traction q(t) as shown in Figure 1. Solution for non-porous media was accomplished by prescribing relative displacement between soil and fluid to be zero.

4.2 QUASI-STATIC PROBLEM OF SOIL CONSOLIDATION

The quasi-static consolidation problem was solved by setting density and damping equal to zero. The example problem selected for cmparison was the one solved earlier by Sandhu (20). Excellent agreement was observed between the present solution and the one obtained (20) using a

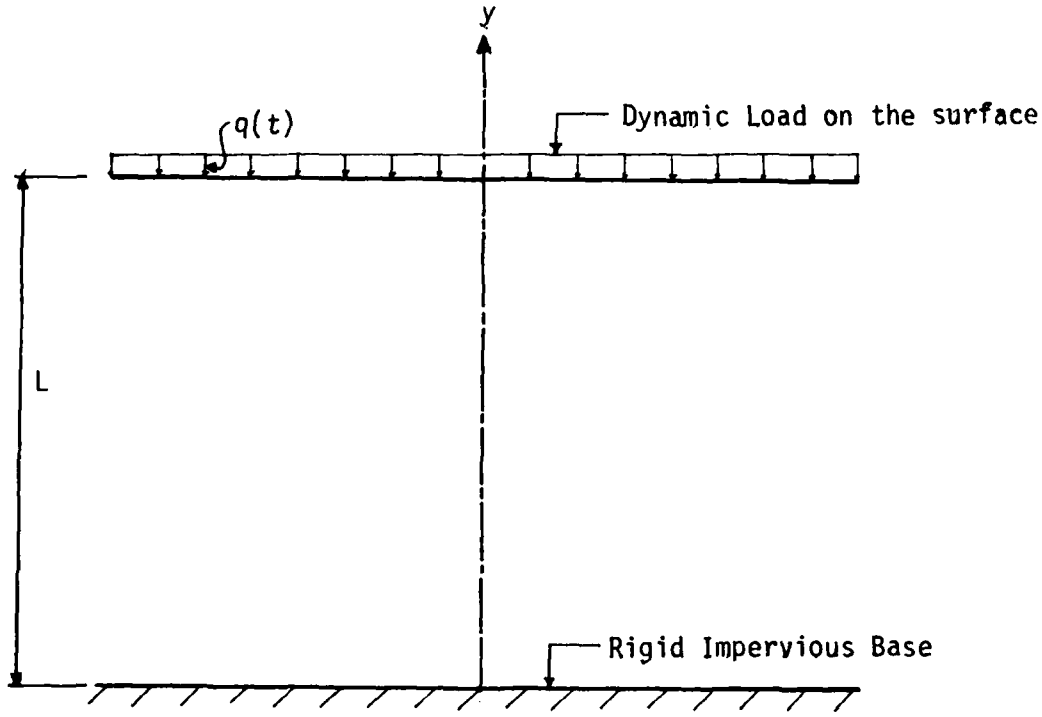

Figure 1: Soil Layer Subjected to Surface Traction

quasi- static consolidation analysis computer program based on the 8-4 element.

4.3 DYNAMIC RESPONSE OF AN ELASTIC BAR OF SINGLE MATERIAL

An elastic layer under spatially uniform excitation applied to its surface can be regarded as an elastic bar, constrained in its lateral dimensions and subjected to excitation at the free end. A representative segment of the layer, equivalent to a laterally restrained bar, is shown in Figure 2. The characteristics used in the finite element model were;

Total length	$L = 500$ mm
Number of nodes	$= 51$
Number of elements	$= 50$
Length of each element	$= 10$ mm
Modulus of elasticity	$E = 20000$ kg/mm^2
Poisson's ratio	$\nu = 0$
Density	$\rho = 0.0008$ kg.m.sec^2/mm^4
Wave velocity	$C_o = [(2\mu + \lambda)/\rho]^{1/2} = 5000$ mm/msec
Time interval	$\Delta t = 0.002$ msec
Number of time steps	$= 50$

where μ, λ are Lame's constants. The following two different conditions at the free end were considered.

a. STEADY STATE RESPONSE

A sinusoidal loading in the form

$$q(t) = q_o \sin(40\pi t) \qquad (19)$$

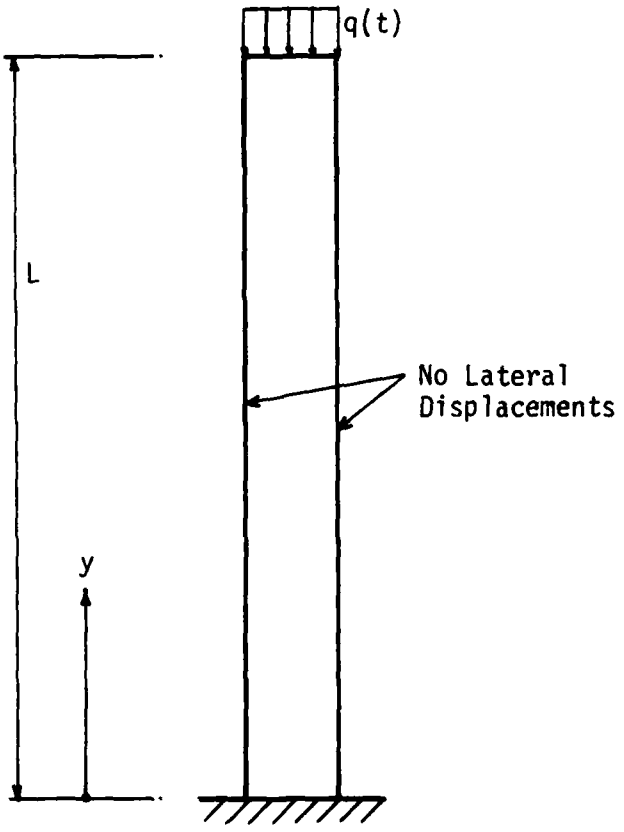

Figure 2: Segment of an Layer Subjected to Dynamic Loading

was applied to one end of the bar with the other end fixed.

b. RESPONSE TO STEP LOAD

A load was suddenly applied and allowed to stay, i.e.

$$q(t) = q_o H(t) = \rho C_o H(t) \tag{20}$$

where H(t) is the Heaviside function. It should be noted that the loading in Equation (20) will induce a unit particle velocity (1). Several values for β, γ, θ were used to obtain the optimum solution. The analytical solution for this problem which contains both the harmonic and the transient solution is given in reference (9).

4.4 RESPONSE OF A FLUID-SATURATED SOIL LAYER (Garg's Problem)

The third example considered was that of a fluid-saturated porous soil layer. The finite element model had the same characteristics as used by Garg (11), i.e.,

Total length	L = 50 cm
Number of nodes	= 51
Number of elements	= 50
Length of each element	= 1 cm
Modulus of elasticity	$E = 0.2319 \times 10^{12}$ dyn/cm^2
Poisson's ratio	$\nu = 0.171$
Mixture mass density	$\rho = 2.3612$ gm/cm^3
Fluid mass density	$\rho_2 = 0.18$ gm/cm^3
Porosity	f = 0.18
Fluid compressibility	$M = 0.102 \times 10^{12}$ dyn/cm^2

Lower bound of wave velocity	C_o = 354875 cm/sec
Upper bound of first kind wave velocity	C_+ = 358193 cm/sec
Upper bound of second kind wave velocity	C_- = 127941 cm/sec

The velocities C_o, C_+, C_- were defined by Biot (2) and Garg (11). Using the notation of this report, these quantities are given by the following expressions (11).

$$C_o^2 = (\lambda + 2\mu + \alpha^2 M)/\rho$$

$$C_1^2 = (\lambda + 2\mu + M(\alpha - f)^2)/\rho_1$$

$$C_2^2 = Mf^2/\rho_2$$

$$C_{12}^2 = Mf(\alpha - f)/\rho_1$$

$$C_{21}^2 = Mf(\alpha - f)/\rho_2$$

$$2C_+^2 = C_1^2 + C_2^2 \pm [(C_1^2 - C_2^2)^2 + 4C_{12}^2 C_{21}^2]^{1/2}$$

Here, $\rho_1 = \rho - \rho_2$ is the bulk mass density of the soil. These velocities are applicable to one-dimensional compressive wave propagation. A unit particle velocity for each phase was imposed at the free surface, i.e.,

$$\dot{u}(L,t) = H(t) \tag{21}$$

$$\dot{w}(L,t) = 0 \tag{22}$$

Equation (22) implies strong coupling at the free surface. In reality, this may not be true. However, for the purpose of comparison with Garg, the same assumptions were made. As reported by Garg et el. (11), as permeability $K \longrightarrow 0$, the relative motion between the two constituents vanishes and phase velocity $C \rightarrow C_0$. This is termed "strong coupling". In this case the material behaves as a single continuum whose properties are combination of those of the two constituents. On the other hand, as $K \longrightarrow \infty$, the coupling between the two constituents vanishes and $C \rightarrow C_+$. This extreme is termed "weak coupling". The boundary condition given by Equation (21) can be replaced by the traction boundary condition, while the boundary conditions expressed by Equation (22) can be replaced by the displacement boundary condition, i.e.

$$q(L,t) = \rho CH(t) \tag{23}$$

$$w(L,t) = 0 \tag{24}$$

where $q(L,t)$ is the traction applied to the free surface. The numerical values for the permeability and the time steps corresponding to strong and weak couplings were;

a. Strong Coupling (Low Permeability)

$K = 0.148 \times 10^{-8}$ cm^3/gm sec

Δt = 1 micro sec

Number of time steps = 50

b. Weak Coupling (High Permeability)

$K = 0.148 \times 10^{-2}$ cm^3/gm sec

Δt = 2.4 micro sec

Number of tme steps = 50

4.5 RESPONSE OF A FLUID-SATURATED SOIL LAYER (Ghaboussi's Problem)

The fourth example was the problem solved by Ghaboussi and Wilson (12). They did not compare the numerical solution with any analytical solution. The problem considered was a fluid-saturated half space subjected to a unit step-loading. The finite element model had the following properties.

Total length	L = 50 cm
Number of nodes	= 51
Number of elements	= 50
Length of each element	= 1 cm
Modulus of elasticity	$E = 0.2319 \times 10^{12}$ dyn/cm^2
Poisson's ratio	$\nu = 0.171$
Mixture density	$\rho = 3$ gm/cm^3
Fluid density	$\rho_2 = 0.18$ gm/cm^3
Porosity	f = 0.18
Fluid compressibility	$M = 90 \times 10^{11}$ dyn/cm^2
Solid compressibilty	$\alpha = 1$
Wave velocity for the mixture (no relative motion)	$C_o = [(2\mu + \lambda + \alpha^2 M)/\rho]^{1/2}$ $= 1.755895 \times 10^6$ cm/sec
Coefficient of permeability	$K = 0.19 \times 10^{-6}$ cm/sec
Time interval	Δt = 1 micro sec

Generally, the solid density of soil falls between the range of 2.0~2.7 (gm/cm^3) and the compressibility of pure water is 2.0×10^{10} (dyn/cm^2). Thus, it should be noted that mixture density and the fluid compressibi-

lity given above are far from real soil properties, but were taken to match the problem solved by Ghaboussi and Wilson (12). Reference (12)did not give any values for k and f. Assigned value of k is for the mixture of very fine sand and silt and f is for very dense state.

SECTION V

RESULTS OF THE ANALYSES

5.1 QUASI-STATIC PROBLEM OF SOIL CONSOLIDATION

The results for the present analysis and those obtained by Sandhu (20) coincided as expected. Detailed results of the analyses were as reported in reference (22) for the problem of one-dimensional consolidation showed using Ghaboussi's 4-4 element.

5.2 DYNAMIC RESPONSE OF AN ELASTIC LAYER OF SINGLE MATERIAL

Figures 3(a) through 3(f) and Table 1(a) thru 1(c) illustrate the stress response of an elastic bar, fixed at one end and subjected to sinusoidal loading at the free end at time stages 0.012, 0.038, 0.05, 0.064, 0.088 and 0.10 seconds. The exact solution (9) for the problem is, for applied load $q(t) = q_o \sin(40\pi t)$,

a. Displacement:

$$u(y,t) = \sum_{n=0} [G(\theta_n) - G(\phi_{n+1})] \tag{25}$$

b. Stress:

$$\sigma(y,t) = -\frac{E}{C_b} \sum_{n=0} [G'(\theta_n) + G'(\phi_{n+1})] \tag{26}$$

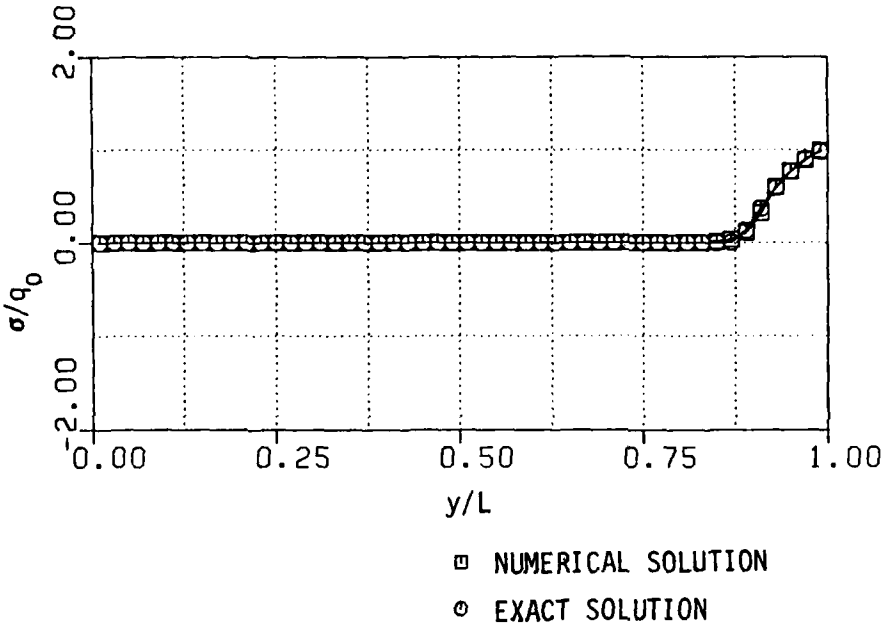

Figure 3: Stress Distribution in an Elastic Layer Subjected to Sinusoidal Load at Free Surface. (a) Time=0.012 second.

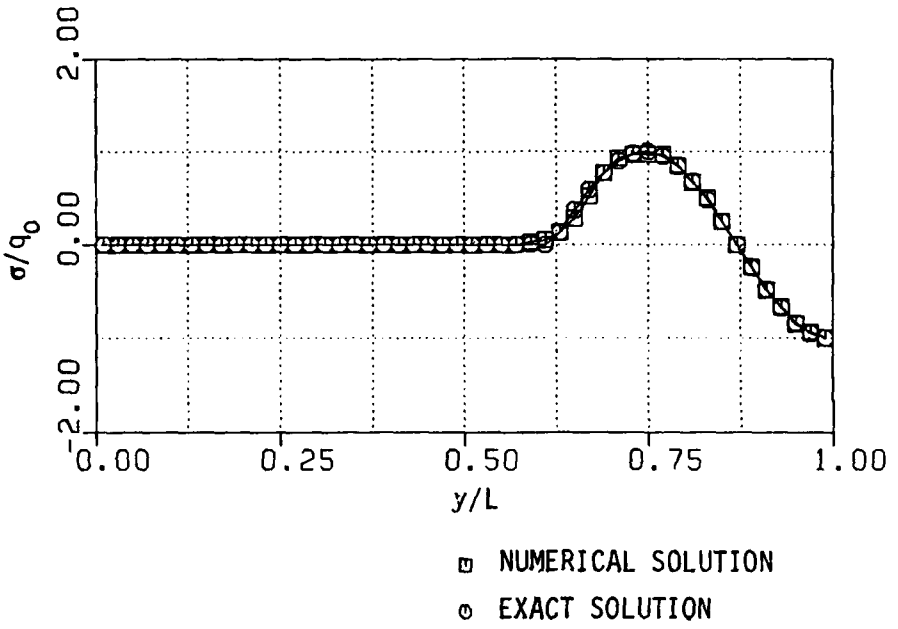

Figure 3: Stress Distribution in an Elastic Layer Subjected to Sinusoidal Load at Free Surface. (b) Time=0.038 second.

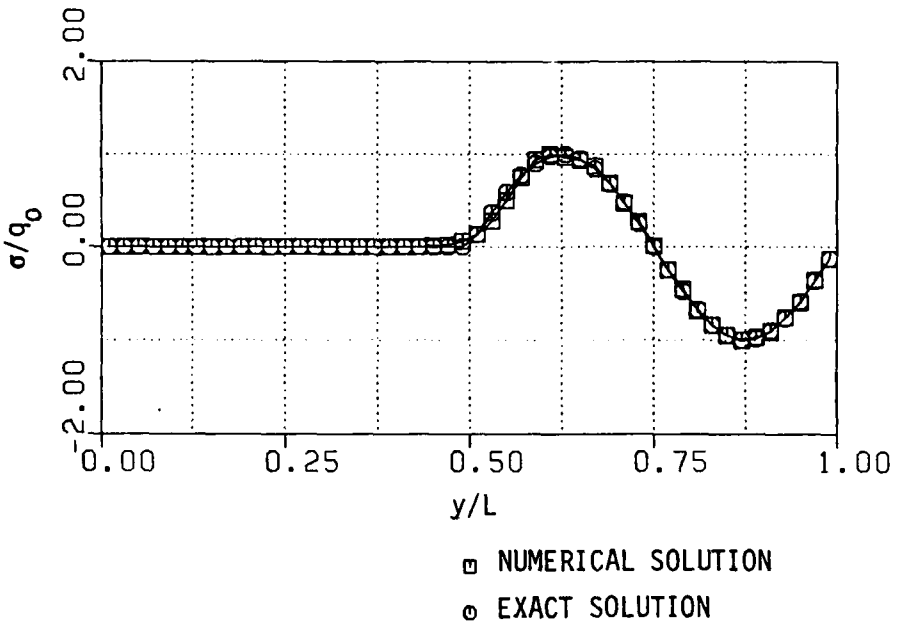

Figure 3: Stress Distribution in an Elastic Layer Subjected to Sinusoidal Load at Free Surface. (c) Time=0.05 second.

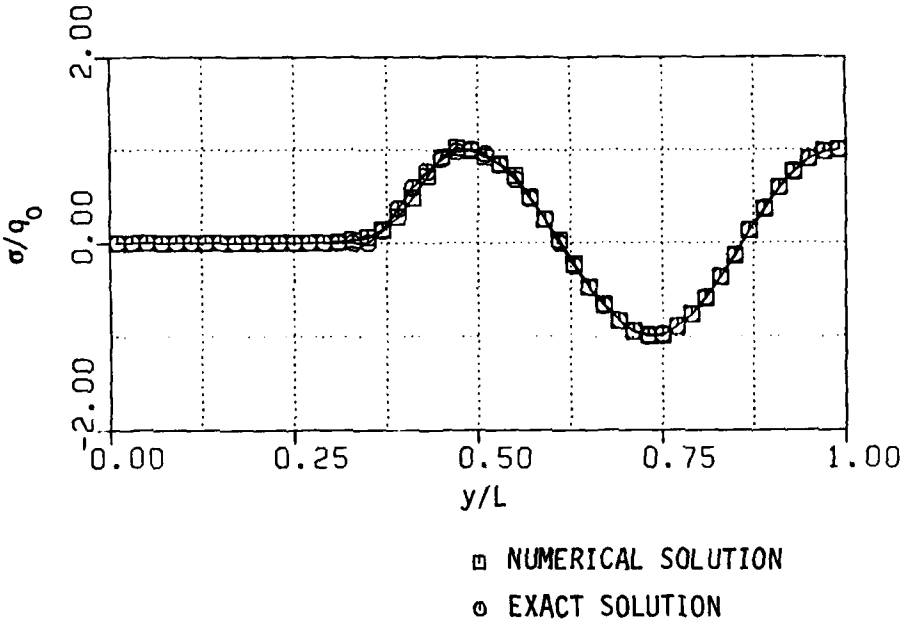

Figure 3: Stress Distribution in an Elastic Layer Subjected to Sinusoidal Load at Free Surface. (d) Time=0.064 second.

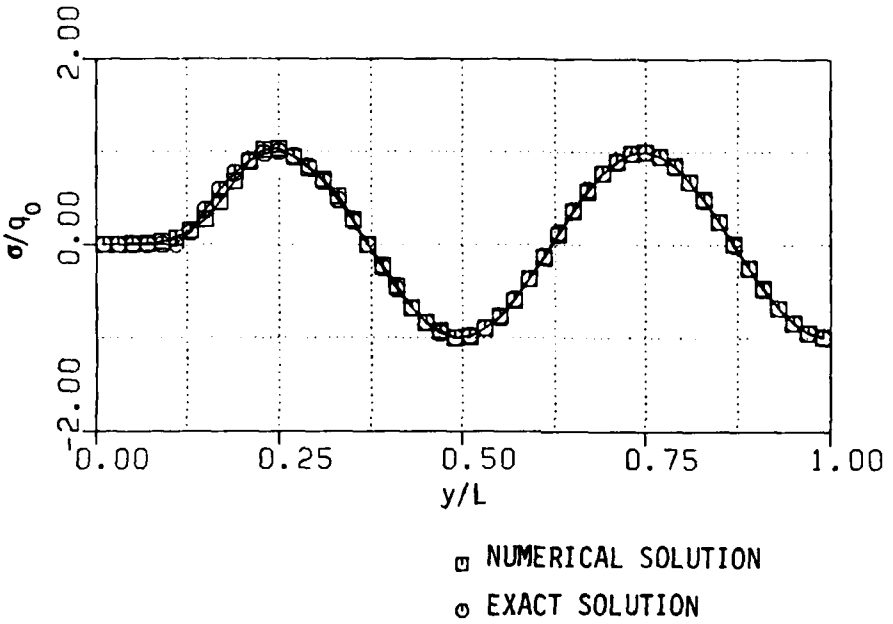

Figure 3: Stress Distribution in an Elastic Layer Subjected to Sinusoidal Load at Free Surface. (e) Time=0.088 second

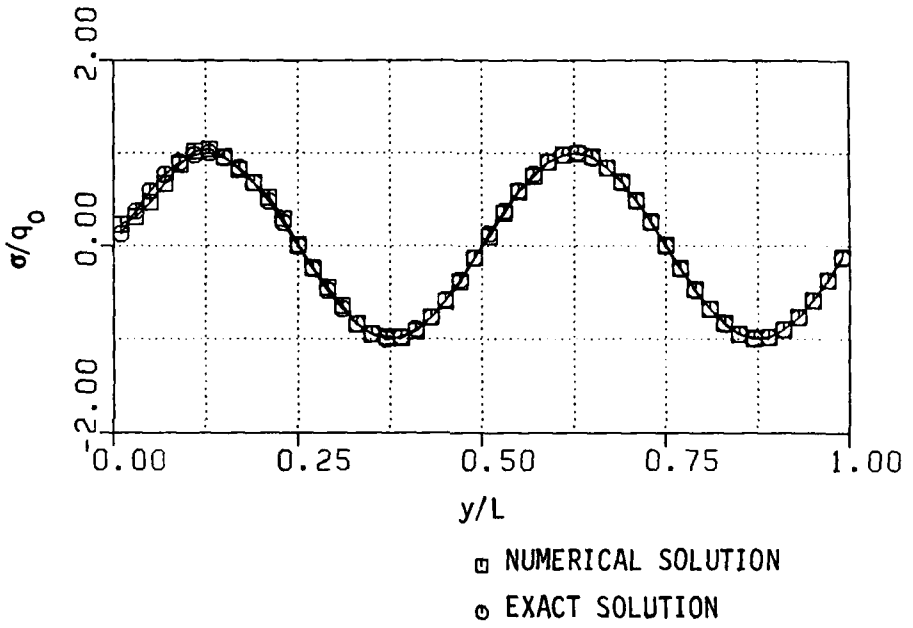

Figure 3: Stress Distribution in an Elastic Layer Subjected to Sinusoidal Load at Free Surface. (f) Time=0.100 second.

TABLE 1

Stress Distribution in an Elastic Layer of Single Material Subjected to Sinusoidal Load at Free Surface. (a) Time= 0.012 and 0.03 second

y/L	σ/q_o			
	t=0.012 sec		t=0.03 sec	
	FEM	EXACT	FEM	EXACT
0.01	0.2349×10^{-45}	0.0	0.2033×10^{-26}	0.0
0.11	0.6543×10^{-40}	0.0	0.1104×10^{-21}	0.0
0.21	0.1835×10^{-34}	0.0	0.4833×10^{-17}	0.0
0.31	0.4703×10^{-29}	0.0	0.1377×10^{-1}	0.0
0.41	0.107×10^{-23}	0.0	0.2132×10^{-8}	0.0
0.51	0.2058×10^{-18}	0.0	0.1297×10^{-4}	0.0
0.61	0.3073×10^{-13}	0.0	0.1581×10^{-1}	0.0
0.71	0.3×10^{-8}	0.0	0.7773	0.7795
0.81	0.1231×10^{-3}	0.0	0.8435	0.8344
0.91	0.3178	0.368	-0.2454	-0.2487
0.99	0.9915	0.9823	-0.9423	-0.9880

TABLE 1

Stress Distribution in an Elastic Layer of Single Material Subjected to Sinusoidal Load at Free Surface. (b) Time= 0.05 and 0.064 second

y/L	σ/q_0			
	t=0.05 sec		t=0.064 sec	
	FEM	EXACT	FEM	EXACT
0.01	0.4820×10^{-18}	0.0	0.3508×10^{-11}	0.0
0.11	0.7783×10^{-14}	0.0	0.1262×10^{-7}	0.0
0.21	0.8188×10^{-10}	0.0	0.2138×10^{-4}	0.0
0.31	0.397×10^{-6}	0.0	0.9445×10^{-2}	0.0
0.41	0.6025×10^{-3}	0.0	0.4798	0.5878
0.51	0.1343	0.1253	0.9235	0.951
0.61	0.9983	0.9823	0.2535×10^{-1}	0.0
0.71	0.4748	0.4828	-0.9523	-0.9510
0.81	-0.6865	-0.6845	-0.5963	-0.5878
0.91	-0.911	-0.9048	0.5883	0.5878
-0.99	-1.3225	-1.2543	0.997	0.9980

TABLE 1

Stress Distribution in an Elastic Layer of Single Material Subjected to Sinusoidal Load at Free Surface. (c) Time= 0.088 and 0.1 second

y/L	σ/q_0			
	t=0.088 sec		t=0.1 sec	
	FEM	EXACT	FEM	EXACT
0.01	0.4158×10^{-5}	0.0	0.2271	0.1253
0.11	0.6543×10^{-2}	0.0	1.0198	0.9823
0.21	0.8933	0.9048	0.5223	0.4818
0.31	0.689	0.6845	-0.6545	-0.6845
0.41	-0.4473	-0.4818	-0.918	-0.9048
0.51	-0.9913	-0.9823	0.1033	0.1253
0.61	-0.1448	-0.1254	0.9768	0.9823
0.71	0.893	0.9048	0.4865	0.4818
0.81	0.6815	0.6845	-0.6838	-0.6845
0.91	-0.4747	-0.4818	-0.901	-0.9048
0.99	-0.994	-0.998	-0.1241	-0.1254

where

$$G(t) = C_b/E \int_0^t q(t)\, dt$$

$$\theta_n = t - (2nL+L-y)/C_b$$

$$\phi_n = t - (2nL-L+y)/C_b$$

$$G'(\zeta) = \frac{dG}{d\zeta}$$

$$G(\theta_n) = 0 \qquad \text{where } \theta_n < 0$$

$$C_b^2 = E/\rho \quad \text{(wave velocity of bar)}$$

The numerical solution was based on values of $q_o = -4$, in addition to those given in section 4.3. The investigation parameters β, γ, θ were set equal to 0.25, 0.5, 1.0, respectively. These values satisfy Equation (16). In Figures 3(a) through 3(f), we see good coincidence between the finite element solution and the analytical solution throughout the spatial as well as the temporal domains. At the point of y/L=0.99, the percentage error at t=0.03 and 0.05 second was 4.6 and 5.4 ,respectively. But at the other time stages it was less than 1.0%.

Figures 4(a) thru 4(c) and Table 2(a) thru 2(c) illustrates the displacement, velocity and stresses along the elastic layer under unit step load at the free surface, at time t = 0.08 sec, i.e. after 40 time increments. The results were obtained for two different time integration

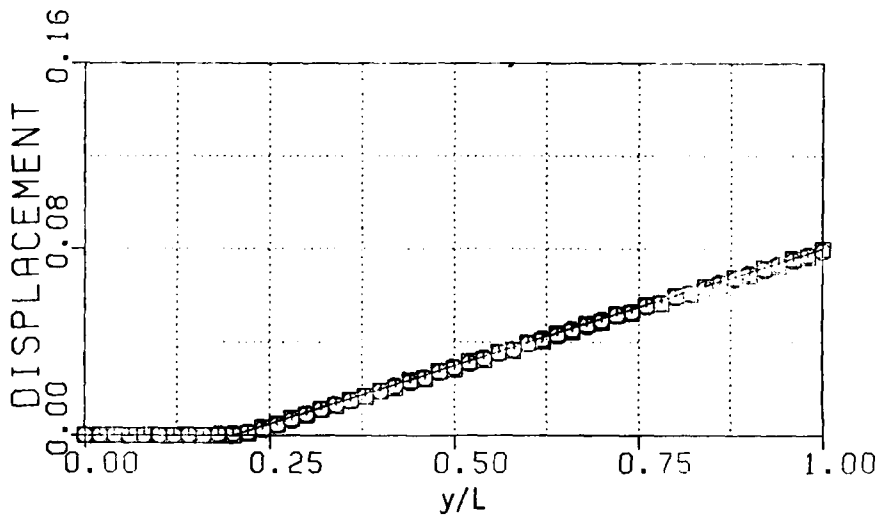

Figure 4: (a) Displacement Distribution in an Elastic Layer under Unit Step Load at Free Surface at Time=0.08 second. Influnece of choice of Parameter β.

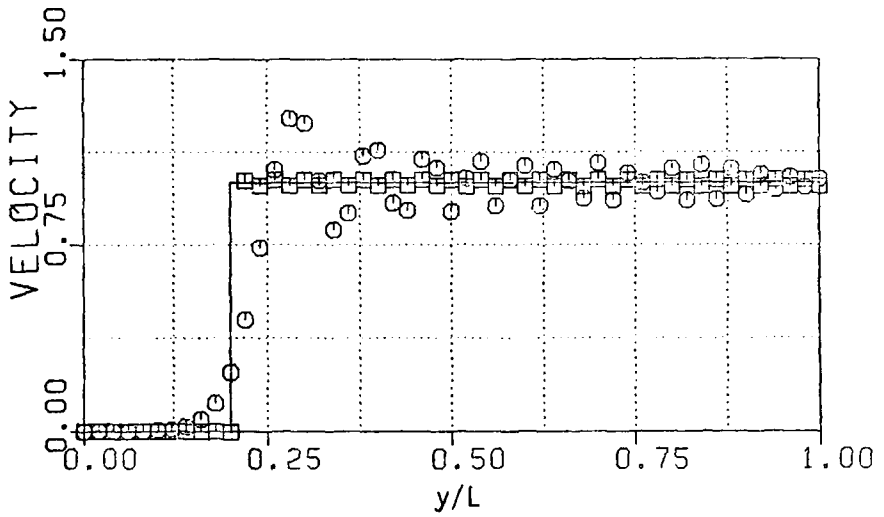

Figure 4: (b) Velocity Distribution in an Elastic Layer under Unit Step Load at Free Surface at Time=0.08 second. Influence of choice of Parameter β.

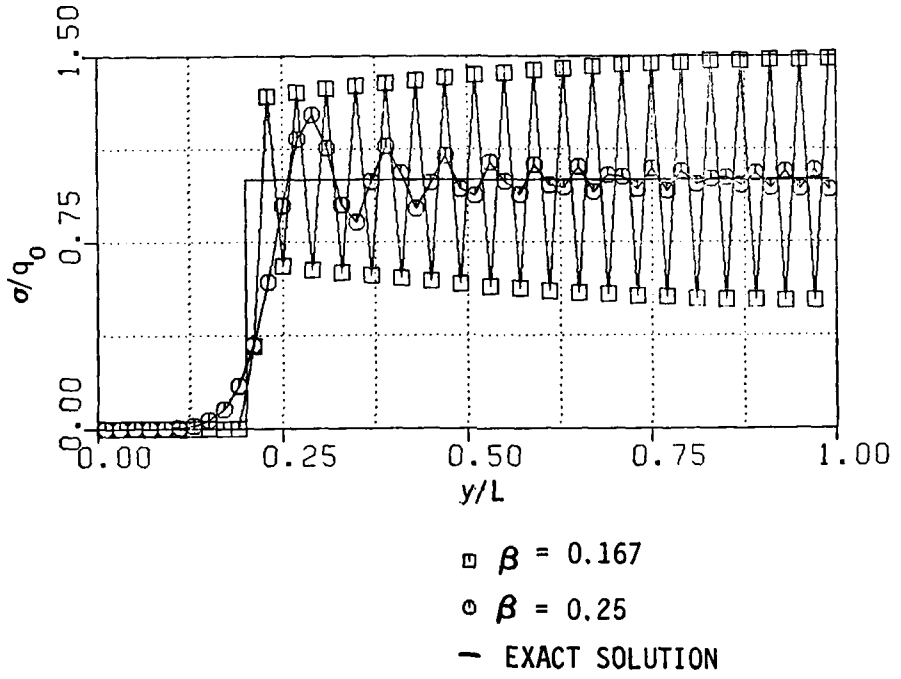

Figure 4: (c) Stress Distribution in an Elastic Layer under Unit Step Load at Free Surface at Time = 0.08 second. Influence of choice of Parameter β.

TABLE 2

(a) Displacement Distribution in an Elastic Layer under Unit Step Load at Time=0.08 sec. Influence of Parameter β.

y/L	β=0.167	β=0.25	EXACT
0.1	0.4811×10^{-21}	4.3568×10^{-5}	0.0
0.2	-0.1785×10^{-5}	6.051×10^{-4}	0.0
0.3	0.008636	0.0091013	0.01
0.4	0.0194	0.001909	0.02
0.5	0.02858	0.02903	0.03
0.6	0.03945	0.03905	0.04
0.7	0.04854	0.04900	0.05
0.8	0.05948	0.05903	0.06
0.9	0.06852	0.06903	0.07
1.0	0.07949	0.07896	0.08

TABLE 2

(b) Velocity Distribution in an Elastic Layer under Unit Step Load at Time=0.08 sec. Influence of Parameter β.

y/L	β=0.167	β=0.25	EXACT
0.1	0.7230×10^{-18}	2.3939×10^{-3}	0.0
0.2	-0.2692	0.2368	0.0
0.3	1.011	1.2398	1.0
0.4	0.9885	1.1337	1.0
0.5	1.0119	0.8844	1.0
0.6	0.9878	1.0681	1.0
0.7	1.0125	1.0813	1.0
0.8	0.9873	1.0582	1.0
0.9	1.0128	0.95322	1.0
1.0	0.9871	1.0168	1.0

TABLE 2

(c) Stress Distribution in an Elastic Layer under Unit Step Load at Time=0.08 sec. Influence of Parameter β.

y/L	σ/q_o		
	β=0.167	β=0.25	EXACT
0.01	0.48×10^{-32}	0.1331×10^{-4}	0.0
0.11	-0.481×10^{-16}	0.4525×10^{-2}	0.0
0.21	0.3333	0.3373	1.0
0.31	1.3673	1.1305	1.0
0.41	0.6023	1.0288	1.0
0.51	1.4245	0.937	1.0
0.61	0.553	0.9803	1.0
0.71	1.4648	1.0113	1.0
0.81	0.5225	0.9808	1.0
0.91	1.4853	1.0275	1.0
0.99	1.4873	0.9618	1.0

schemes and compared with analytical solution (1,9). The first scheme used $\theta = 1.0$, $\beta = 0.5$, $\gamma = 0.167$, and the second $\theta = 1.0$, $\beta = 0.5$, $\gamma = 0.25$. It is shown from Figure 4 Table 2(a) that both schemes give the almost same displacement response with about 3 error against the exact solution. However, $\beta = 0.167$ was better for velocity and $\beta = 0.25$ better for stress distribution. Despite this fact, large error around wave front was still observed and numerical results were not reliable. The oscillatory error may be overcome by increasing γ and using the corresponding value of β from Equation (17) as we shall see in the next example. For this problem, one-dimensional linear element (called 1-1 element) was used and CPU time on the AMDAHL 470/V8 Computer was 15.18 seconds for sinusoidal loading and 15.4 seconds for unit step loading, respectively.

5.3 RESPONSE OF A FLUID-SATURATED SOIL LAYER (Garg's Problem)

In order to investigate the effect of fluid-soil interaction on wave propagation, two different values of the permeability coefficient were selected to approximate "strong" and "weak" coupling extremes described by Garg (11). Figures 5(a) and 5(b) and Table 3(a) and 3(b) show the velocity for both the solid and the fluid at 10cm from the traction boundary. The numerical results are based on calculations with $\theta = 1$, $\beta = 0.6$, $\gamma = 0.3025$. Reasonable agreement is seen between the finite element and the analytical solutions. But while the exact solution has the sharp discintinuity in the wave front, numerical was diffused. A single wave front exists. The wave is propagating with velocity = C_0, and the solid velocity is the same as the fluid velocity. This is because, for this

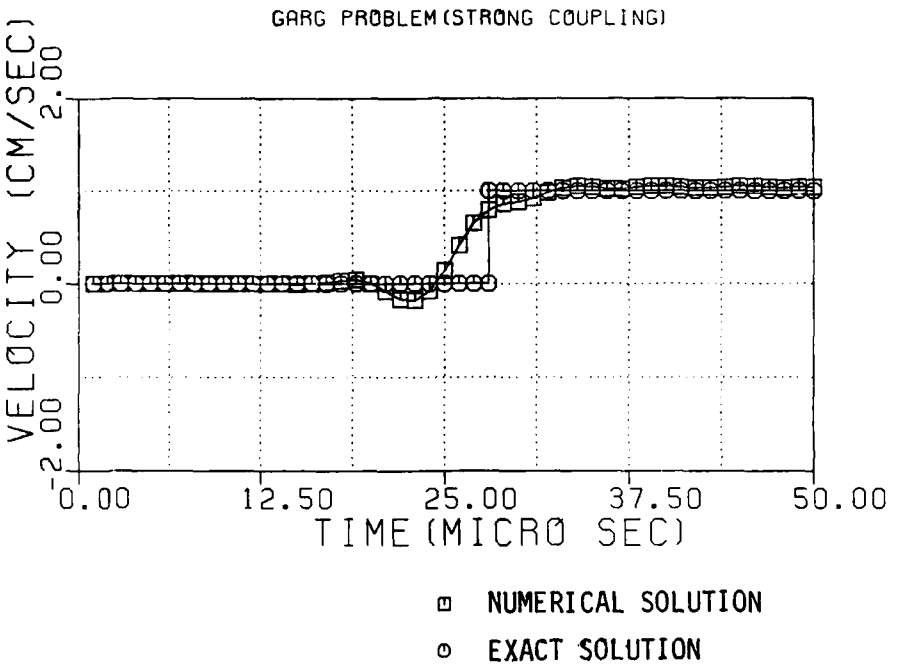

Figure 5: (a) Garg's Problem for Strong Coupling; Velocity History of the solid at 10cm from the Tractron Boundary.

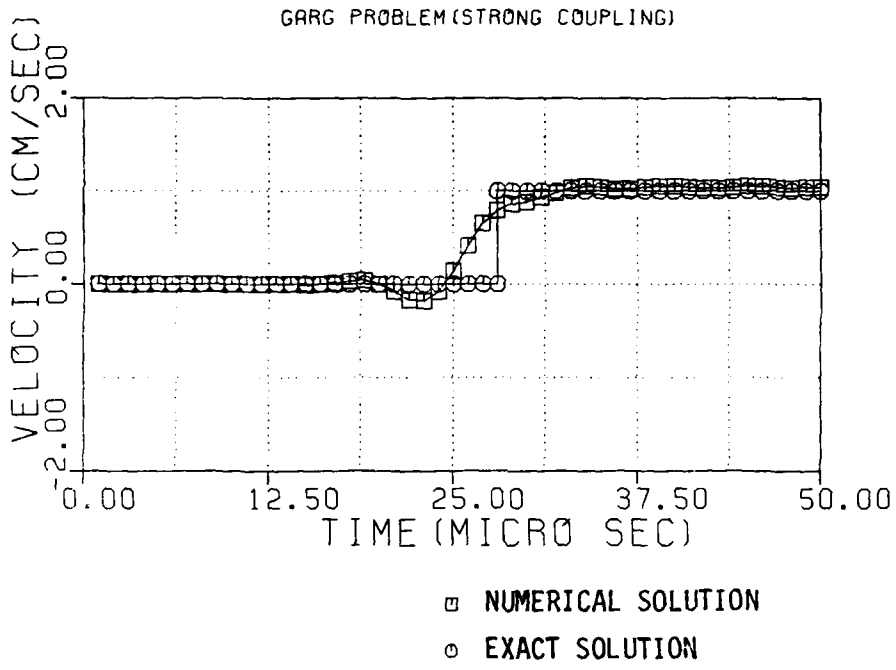

Figure 5: (b) Garg's Problem for Strong Coupling; Velocity History of the Fluid at 10cm from the Traction Boundary.

TABLE 3

Velocity History of Garg's Problem at 10cm from the Traction Boundary for Strong Coupling.

Time	Solid (cm/sec)		Fluid (cm/sec)	
(sec)	FEM	EXACT	FEM	EXACT
0.001	0.1479×10^{-7}	0.0	-0.1479×10^{-7}	0.0
0.01	0.1479×10^{-3}	0.0	-0.1479×10^{-3}	0.0
0.015	-0.7322×10^{-2}	0.0	-0.7322×10^{-2}	0.0
0.02	-0.1861×10^{-2}	0.0	-0.1861×10^{-2}	0.0
0.025	-0.1888	0.0	-0.1888	0.0
0.026	0.4125	0.0	0.4125	0.0
0.027	0.6484	0.0	0.6484	0.0
0.028	0.7939	0.0	0.7939	0.0
0.030	0.8848	1.0	0.8848	1.0
0.035	1.0366	1.0	1.0366	1.0
0.040	1.0546	1.0	1.0546	1.0
0.045	1.0505	1.0	1.0505	1.0
0.050	1.0434	1.0	1.0434	1.0

problem, relative velocity w approaches zero and the two constituents effectively act as a single continuum.

Figures 6(a) and 6(b) demonstrate the results of other extreme viz. "weak" coupling. The values of θ, γ, β were the same as for the "strong" coupling. The results for a station 10 cm away from traction boundary (y = 40cm) are quite close to Garg's analytical solution (11). Existence of two wave fronts travelling with speeds C_- and C_+ is noticed.

Pore pressure distribution at different times for the two extremes of "strong" and "weak" coupling are plotted in Figure 7(a) and 7(b). A single phase description is seen in Figure 7(a), in which the pressure wave is propagating with speed C_τ. Figure 7(b) clearly demonstrates the existence of two waves travelling with speed C_- and C_+, in the fluid and the solid, respectively. The above results were obtained by 1-1 element. CPU time was 15.68 seconds for weak coupling analysis and 15.4 seconds for strong coupling.

5.4 RESPONSE OF A FLUID-SATURATED SOIL LAYER (GHABOUSSI'S PROBLEM)

Figure 8 presents the response of a saturated layer to a unit step loading. Solution of this problem was attempted by Ghaboussi and Wilson (12). However, their results, were criticized by Garg (11), and do not agree with the plot in Figure 8 (Table 5). In this figure, the non-dimensional pore pressure π/q_o is plotted against $y^* = y/(KC_o)$. For $\alpha = 1$ and $M \rightarrow \infty$ the pore pressure should be equal to the applied traction. Ghaboussi and Wilson (12) reported figures which do not match Figure 8. With 1-1 element, CPU time for the problem was 12.35 seconds.

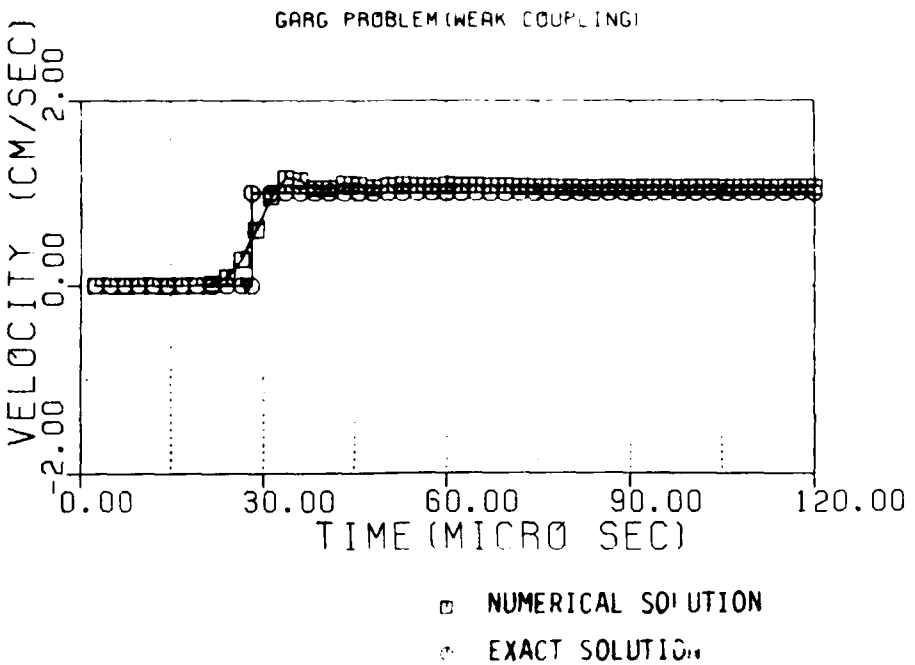

Figure 6: (a) Garg's Problem for Weak Coupling; Velocity History of the Solid at 10cm from the Traction Boundary.

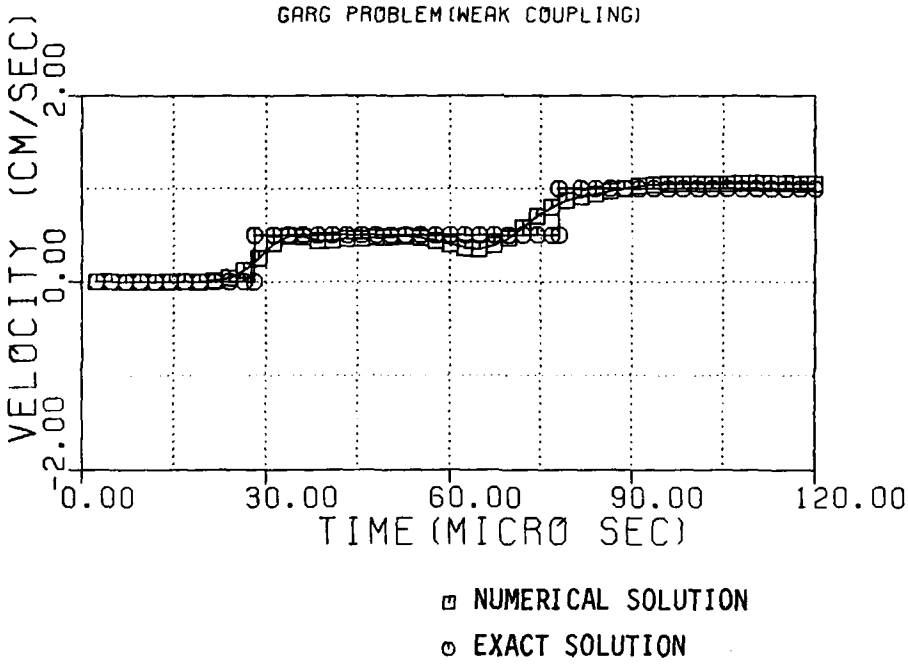

Figure 6: (b) Garg's Problem for Weak Coupling; Velocity History of the Fluid at 10cm from the Traction Boundary.

TABLE 4

Velocity History of Garg's Problem at 10cm from the Traction Boundary for Weak Coupling.

Time	Solid (cm/sec)		Fluid (cm/sec)	
(sec)	FEM	EXACT	FEM	EXACT
0.0024	-0.2009×10^{-8}	0.0	-0.5264×10^{-7}	0.0
0.0096	0.1844×10^{-6}	0.0	-0.1150×10^{-5}	0.0
0.0192	0.4323×10^{-2}	0.0	0.1890×10^{-2}	0.0
0.0312	0.9575×10^{-2}	1.0	0.4078	0.5
0.0408	1.0527	1.0	0.4428	0.5
0.0504	1.0760	1.0	0.4834	0.5
0.060	1.0856	1.0	0.4880	0.5
0.696	1.0807	1.0	0.4720	0.5
0.0792	1.0632	1.0	0.8662	1.0
0.0912	1.0577	1.0	1.0260	1.0
0.1008	1.0568	1.0	1.0475	1.0
0.1104	1.0560	1.0	1.0555	1.0
0.120	1.0562	1.0	1.0549	1.0

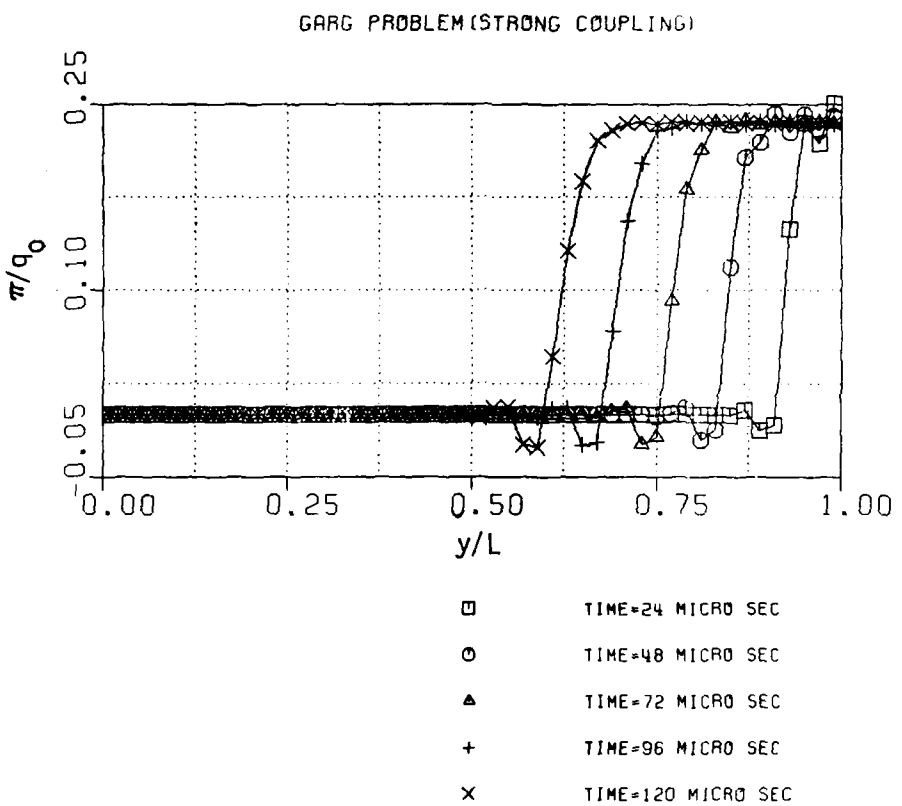

Figure 7: Pore Pressure Distribution at Various Times for Garg's Problem. (a) Strong Coupling.

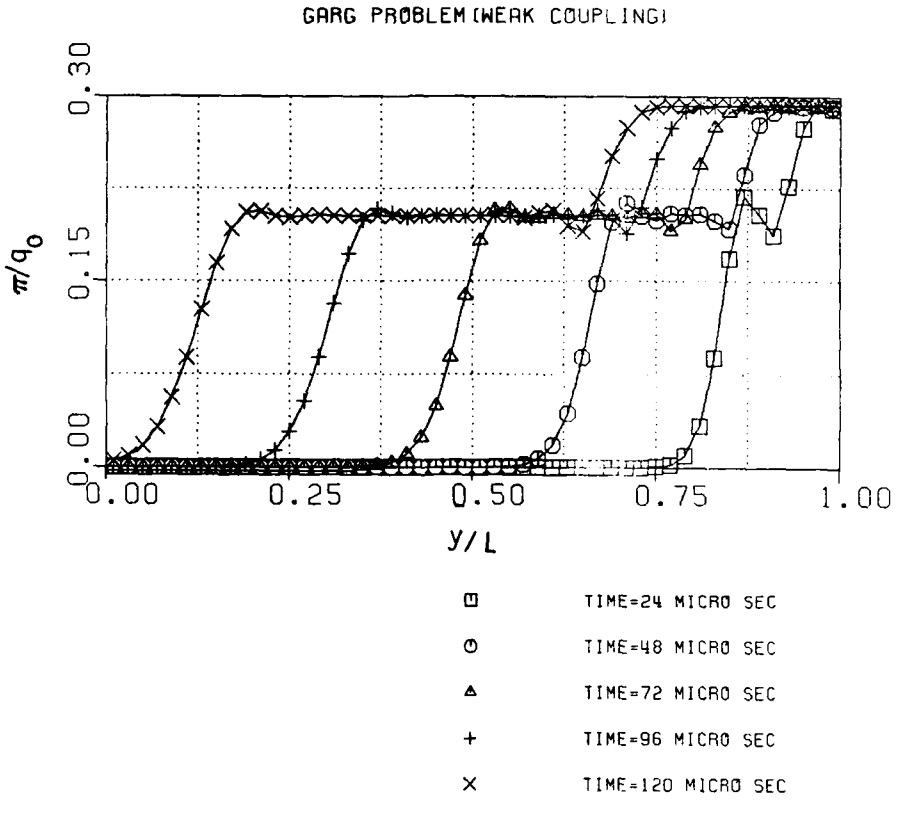

Figure 7: Pore Pressure Distribution at Various times for Garg's Problem; (b) Weak Coupling.

TABLE 5

Pore Pressure (π/q_0) Distribution of Garg's Problem

y/L	Strong Coupling (t=0.05 milli sec)	Weak Coupling (t=0.12 milli sec)
0.01	-0.1332×10^{-14}	0.5204×10^{-2}
0.11	-0.1296×10^{-11}	0.8856×10^{-1}
0.21	-0.9494×10^{-9}	0.2026
0.31	-0.1544×10^{-6}	0.2031
0.41	-0.3558×10^{-4}	0.2027
0.51	-0.2315×10^{-2}	0.2027
0.61	-0.4647×10^{-1}	0.2070
0.71	0.2345	0.2747
0.81	0.2359	0.2928
0.91	0.2344	0.2928
0.99	0.2347	0.2928

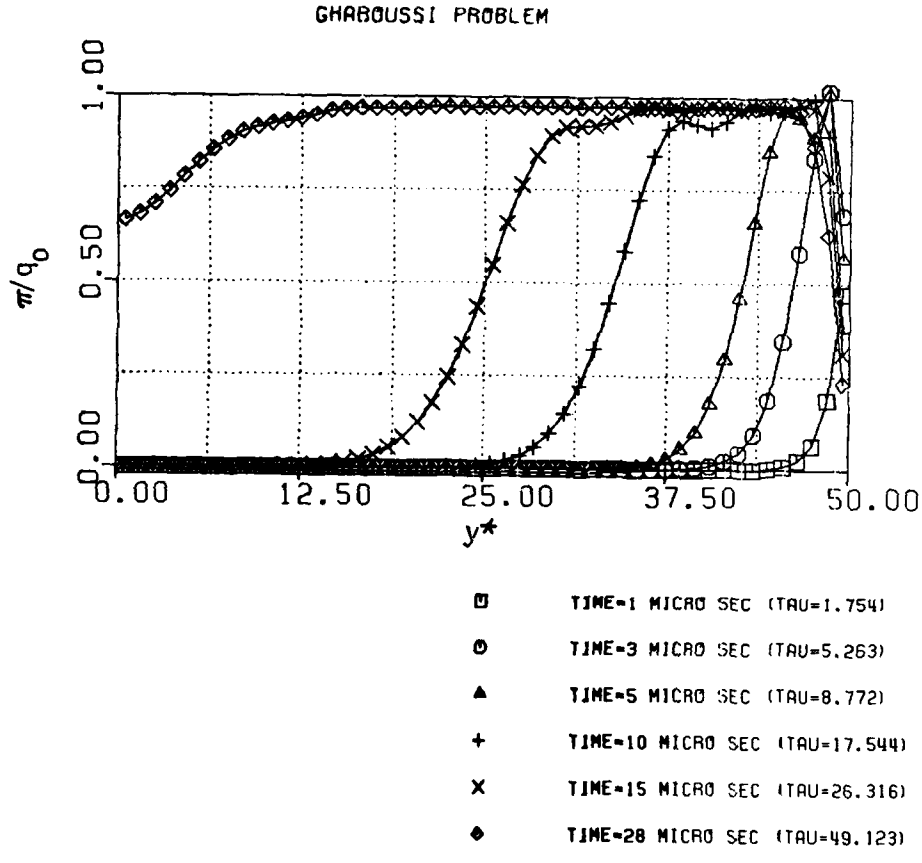

Figure 8: Pore Pressure Distribution History for Ghaboussi's Problem.

TABLE 6

Pore Pressure Distribution (π/q_0) of Ghaboussi's Problem at Time=0.111, 0.015 and 0.028 milli second

y/L	t=0.111	t=0.015	t=0.028
0.01	2.235×10^{-22}	2.428×10^{-6}	0.6653
0.11	2.651×10^{-20}	4.328×10^{-5}	0.8208
0.21	4.108×10^{-18}	8.997×10^{-4}	0.9243
0.31	6.364×10^{-16}	1.33×10^{-2}	0.9648
0.41	9.861×10^{-14}	1.217×10^{-1}	0.9706
0.51	1.518×10^{-11}	5.473×10^{-1}	0.9721
0.61	2.367×10^{-9}	9.179×10^{-1}	0.9729
0.71	3.667×10^{-7}	9.703×10^{-1}	0.9733
0.81	5.692×10^{-5}	9.776×10^{-1}	0.9729
0.91	8.712×10^{-3}	9.678×10^{-1}	0.9771
0.99	0.4728	3.123×10^{-1}	0.2330

SECTION VI

CONCLUSIONS

Galerkin finite element method was used along with the β-γ-θ algorithm to set up numerical scheme for investigating wave propagation through saturated porous media. Several problems with known analytical solutions were analyzed. Results of the analyses indicate the following:

1. The integration parameters β, γ and θ should be carefully selected to avoid oscillatory error.

2. The scheme, with proper selection of β, γ and θ, showed exellent agreement with the analytical solutions.

3. The numerical and analytical results show the importance of the role of permeability in single or double phase description for fluid-saturated porous media. For low permeability, there is little relative motion and the strong coupling on single material description would be valid. For high permeability, the two phase description is necessary.

4. The computer code was checked only for one-dimensional problems. Its effectivenes for two-dimensional (plane strain) problems is yet to be established.

5. Further investigation in the choice of damping matrices is required. The solution process for a few idealized problems has been checked, but the assumptions regarding various couplings may not represent actual soil behavior.

6. The computer code implemented Ghaboussi and Wilson's version of Biot's theory. The entire fluid mass is expected to be in relative motion. In other theories, an interaction mass is introduced. This would imply a "partial" coupling somewhere between the "strong" and "weak" coupling defined by Garg (11). Work is needed to quantify the coupling and to allow for this in the computer code by suitably defining mass matrices.

7. The computer code needs to be extended to propagation of shear waves and Love and Rayleigh waves. Studies are needed to allow for reflection and refraction of waves at interfaces or boundaries. Dynamics of nonhomogeneous, anisotropic and nonlinear soils needs to be investigated.

REFERENCES

1. Achenbach, J.D.; 1973, Wave Propagation in Elastic Solids, North-Holland Publishing Company, Amsterdam, New York, Oxford.

2. Biot, M.A.; 1956, "Theory of Propagation of Elastic Waves in a Fluid Saturated Porous Solid, I. Low-Frequency Range", J. the Acous. Soc. Amer., 28, No.2, 168-178.

3. Biot, M.A.; 1961, "Mechanics of Deformation and Acoustic Propagation in Porous Media", J. Appl. Phys., 33, No.4, 1483-1498.

4. Chakraborty, S.K., and Dey, S.; 1982, "The Propagation of Love Waves in Water-Saturated Soil Underlain by Heterogeneous Elasic Medium", Acta Mechanica, 44, 169-176.

5. Clough, R.W., and Penzien, J.; 1975, Dynamics of Structures, McGraw-Hill, New York, N.Y.

6. Deresiewicz, H.; 1960, "The Effect of Boundaries on Wave Propagation in a Liquid-filled Porous Solid: I. Reflection of Plane Waves at a Free Plane Boundary (Non-Dissipate Case)", Bull. Seis. Soc. Amer., 50, 599-607.

7. Deresiewicz, H.; 1960, "The Effect of Boundaries on Wave Propagation in a Liquid-filled Porous Solid: II. Love Waves in a Porous Layer", Bull. Seis. Soc. Amer., 51, 51-59.

8. Desai, C.S.; 1979, Elementary Finite Element Method, Prentice-Hall, New Jersey.

9. Flugge, W.; 1966, Handbook of Engineering Mechanics, McGraw-Hill, New york, N.Y.

10. Garg, S.K.; 1971, "Wave Propagation Effects in a Fluid-Saturated Porous Solid", J. Geophy. Res., 76, 7947-7962.

11. Garg, S.K., Nayfeh, A.H., and Good, A.J.; 1974, "Compressional Waves in Fluid-Saturated Elastic Porous Media", J. Appl. Phys., 45, 1968-1974.

12. Ghaboussi, J., and Wilson, E.L.; 1973, "Variational Formulation of Dynamics of Fluid Saturated Porous Elastic Solids", Amer. Soc. Civ. Engrs., 98, J. Engrg. Mech. Div., 947-963.

13. Hsieh, L., and Yew, C.H.; 1973, "Wave Motions in a Fluid Saturated Porous Medium", J. Appl. Mech., 40, 873-878.

14. Hughes, T.J.R., Pister, K.S., and Taylor, R.L.; 1979, "Implicit-Explicit Finite Elements in Nolinear Transient Analysis", Comp. Meth. Appl. Mech. Engrg., 17/18, 159-182.

15. Ishihara, K.; 1967, "Propagation of Compressional Waves in a Saturated Solid", Proc. Int. Symp. on Wave Propagation and Dynamic Properties of Earth Materials, Univ. of New Mexico Press, Albuquerque, 451-467.

16. Newmark, N.M., 1959, "A Method for Computation for Structural Dynamics", Am. Soc. Civ. Engrs., 85, J. Engrg Mech. Div., 67-94.

17. Prevost, J.H.; 1982, "Nonlinear Transient Phenomena in Saturated Porous Media", Comp. Meth. Appl. Mech. Engrg., 30, 3-18.

18. Sandhu, R.S.; 1968, Fluid Flow in Saturated Porous Media, Ph.D. Thesis, University of California, Berkeley, California.

19. Sandhu, R.S., and Pister, K.S.; 1970, "A Variational Principle for Linear Coupled Field Problems in Continuum Mechanics", Int. J. Engrg. Sci., 8, 989-999.

20. Sandhu, R.S.; 1976, Finite Element Analysis of Soil Consolidation, Report OSURF-3570-76-3 to National Science Foundation, Dept. of Civil Engineering, The Ohio State University, Columbus, Ohio.

21. Sandhu, R.S.; 1982, "Finite Element Analysis of Subsidence due to Fluid Withdrawal", Forum on Subsidence due to Fluid Withdrawal, Fountainhead State Resort, Oklahoma.

22. Aboustit, B.L., and Sandhu, R.S.; 1984, An Evaluation of Finite Element Methods for Soil Consolidation, Report OSURF-715107-84-2 to Air Force Office of Scientific Research, Dept. of Civil Engineering, The Ohio State University, Columbus, Ohio.

23. Zienkiewicz, O.C.; 1979, The Finite Element Method, 3rd Ed., McGraw-Hill, London.

24. Zienkiewicz, O.C., Chang, C.T., and Bettess, P.; 1979, Drained, Undrained Consolidation and Dynamic Behavior Assumptions in Soils, Limits of Validity, Report C/R/349/79, University College of Swansea, Wales, U.K., SA2899.

Appendix A

SPATIAL DISCRETIZATION

In this appendix, we present the spatial discretization of the equation of wave propagation through saturated porous media using Galerkin's method.

A.1 WEAK FORMULATION

A weak form for Equation (1) is;

$$\int_V [E_{ijkl} u_{k,lj} + \alpha M \delta_{ij} (\alpha u_{k,k} + w_{k,k})_{,j} + \rho f_i - \rho \ddot{u}_i - \frac{1}{f} \rho_2 \ddot{w}_i] \psi^M dv = 0 \qquad (A\text{-}1)$$

where ψ^M is a test function. Equation (A-1) can be rewritten as

$$\int_V [(E_{ijkl} u_{k,l} \psi^M)_{,j} - E_{ijkl} u_{k,l} \psi^M_{,j} + (\alpha^2 M \delta_{ij} u_{k,k} \psi^M)_{,j} - \alpha^2 M \delta_{ij} u_{k,k} \psi^M_{,j} + (\alpha M \delta_{ij} w_{k,k} \psi^M)_{,j} - \alpha M \delta_{ij} w_{k,k} \psi^M_{,j} + (\rho f_i - \rho \ddot{u}_i - \frac{1}{f} \rho_2 \ddot{w}_i) \psi^M] dv = 0 \qquad (A\text{-}2)$$

Using Gauss theorem on the first, the third and the fifth terms,

$$\int_S [E_{ijkl} u_{k,l} + \alpha^2 M \delta_{ij} u_{k,k} + \alpha M \delta_{ij} w_{k,k}] \psi^M n_j \, dS + \int_v \rho f_i \psi^M dv$$

$$= \int_v [E_{ijkl} u_{k,l} \psi^M_{,j} + \alpha^2 M \delta_{ij} u_{k,k} \psi^M_{,j} + \alpha M \delta_{ij} w_{k,k} \psi^M_{,j}$$

$$+ (\rho \ddot{u}_i + \frac{1}{f} \rho_2 \ddot{w}_i) \psi^M] \, dv \qquad \text{(A-3)}$$

where n_i are the components of the outward unit normal to S. The total stress tensor is defined as (4)

$$\tau_{ij} = E_{ijkl} u_{k,l} + \alpha^2 M \delta_{ij} u_{k,k} + \alpha M \delta_{ij} w_{k,k} \qquad \text{(A-4)}$$

Hence, Equation (A-3) can be rewritten as

$$\int_S \tau_{ij} n_j \psi^M \, dS + \int_v f_i \psi^M \, dv$$

$$= \int_v [E_{ijkl} u_{k,l} \psi^M_{,j} + \alpha^2 M \delta_{ij} u_{k,k} \psi^M_{,j} + \alpha M \delta_{ij} w_{k,k} \psi^M_{,j}$$

$$+ (\rho_1 \ddot{u}_i + \frac{1}{f} \rho_2 \ddot{w}_i) \psi^M] \, dv \qquad \text{(A-5)}$$

From the boundary conditions, Equations (3) and (4), we have

$$\psi^M = 0 \qquad \text{on } S_{1i} \qquad \text{(A-6)}$$

$$\tau_{ij} n_j = \hat{t}_i \qquad \text{on } S_{2i} \qquad \text{(A-7)}$$

Substituting Equations (A-6) and (A-7) into Equation (A-5),

$$\int_{S_{2i}} \hat{t}_i \psi^M \, dS + \int_v f_i \psi^M \, dv = \int_v [E_{ijkl} u_{k,l} \psi^M_{,j} + (\alpha^2 M \delta_{ij} u_{k,k} \psi^M_{,j}$$

$$+ \alpha M \delta_{ij} w_{k,k} \psi^M_{,j} + (\rho \ddot{u}_i + \tfrac{1}{f} \rho_2 \ddot{w}_i) \psi^M] \, dv \qquad \text{(A-8)}$$

Similarly, a weak form for Equation (2) is

$$0 = \int_v [M(\alpha u_{k,k} + w_{k,k})_{,i} + \tfrac{1}{f} \rho_2 f_i - \tfrac{1}{f} \rho_2 \ddot{u}_i - \tfrac{1}{f^2} \rho_2 \ddot{w}_i - C_{ij} \dot{w}_j] \phi^M \, dv \qquad \text{(A-9)}$$

where ϕ^M is a test function. Equation (A-9) can be rewritten as

$$\int_v [(M(\alpha u_{k,k} + w_{k,k}) \phi^M)_{,i} - M(\alpha u_{k,k} + w_{k,k}) \phi^M_{,i}$$

$$+ \tfrac{1}{f} \rho_2 f_i - \tfrac{1}{f} \rho_2 \ddot{u}_i - \tfrac{1}{f^2} \rho_2 \ddot{w}_i - C_{ij} \dot{w}_j] \phi^M \, dv = 0 \qquad \text{(A-10)}$$

Noting that the pore pressure is given by (3) as

$$\pi = M(\alpha u_{i,i} + w_{i,i}) \qquad \text{(A-11)}$$

and using Gauss theorem on the first term, Equation (A-10) can be written as

$$\int_S \pi n_i \phi^M \, dS + \int_v \tfrac{1}{f} \rho_2 f_i \phi^M \, dv$$

$$= \int_v [M(\alpha u_{k,k} + w_{k,k}) \phi^M_{,i} + (\tfrac{1}{f} \rho_2 \ddot{u}_i + \tfrac{\rho_2}{f^2} \ddot{w}_i + C_{ij} \dot{w}_j) \phi^M] \, dv \qquad \text{(A-12)}$$

where n_i are components of the outward unit normal to S. Equations (5) and (6) for $\hat{\pi} = 0$ are

$$\phi^M = 0 \qquad \text{on } S_4 \tag{A-13}$$

$$\pi n_j = \hat{\pi} n_j \qquad \text{on } S_3 \tag{A-14}$$

Hence, Equation (A-12) may be written as

$$\int_{S_3} \hat{\pi} n_i \, \phi^M \, dS + \int_v \frac{1}{f} \, \rho_2 f_i \, \phi^M \, dv$$

$$= \int_v [M(\alpha \, u_{k,k} + w_{k,k}) \, \phi^M_{,i} + (\frac{1}{f} \, \rho_2 \ddot{u}_i + \frac{\rho_2}{f^2} \ddot{w}_i + C_{ij} \dot{w}_j) \, \phi^M] \, dv \tag{A-15}$$

A.2 GALERKIN APPROXIMATION

For a typical element, the local solid and relative fluid displacements are approximated by

$$u_i = \psi^N(x) \, u_i^N \tag{A-16}$$

$$w_i = \phi^N(x) \, w_i^N \tag{A-17}$$

where ψ^N and ϕ^N are interpolating functions defined over the finite element and u_i^N, w_i^N are the values of solid and fluid displacements at the node N.

Substituting from Equation (A-16), (A-17) into Equation (A-8) gives

$$\int_{S_{2i}} \hat{t}_i \, \psi^M \, dS + \int_v \rho f_i \, \psi^M \, dv$$

$$= \int_v [E_{ijkl} \, \psi^N_{,l} \, u_k^N \, \psi^M_{,j} + \alpha^2 \, M \, \delta_{ij} \psi^N_{,k} \, \psi^M_{,j} \, u_k^N$$

$$+ \alpha M \delta_{ij} \phi^N_{,k} w^N_k \psi^M_{,j} + (\rho \psi^N \ddot{u}_i + \frac{1}{f} \rho_2 \phi^N \ddot{w}_i) \psi^M] \, dv \qquad \text{(A-18)}$$

Define

$$\int_{S_{2i}} \hat{t}_i \psi^M \, dS + \int_v f_i \psi^M \, dv = F^M_{si}$$

$$\int_v [E_{ijkl} \phi^N_{,l} \psi^M_{,j} + \alpha^2 M \delta_{ij} \psi^M_{,j} \psi^N_{,k}] \, dv = K^{NM}_{ssik}$$

$$\int_v \alpha M \delta_{ij} \psi^N_{,k} \psi^M_{,j} \, dv = K^{NM}_{sfik} \qquad \text{(A-19)}$$

$$\int_v \rho \psi^N \psi^M \, dv = M^{NM}_{ss}$$

$$\int_v \frac{1}{f} \rho_2 \phi^N \psi^M \, dv = M^{NM}_{sf}$$

Substituting Equation (A-19) into (A-18),

$$K^{NM}_{ssik} u^N_k + K^{NM}_{sfik} w^N_k + M^{NM}_{ss} \ddot{u}^N_i + M^{NM}_{sf} \ddot{w}^N_i = F^M_{si} \qquad \text{(A-20)}$$

Similarly, substituting from Equation (A-16),(A-17) into Equation (A-15)

$$\int_{S_3} \phi^M \hat{\pi} n_i \, dS + \int_v \frac{1}{f} \rho_2 f_i \phi^M \, dv$$

$$= \int_v M \alpha \psi^N_{,k} \phi^M_{,i} u^N_k + \int_v M \phi^N_{,k} \phi^M_{,i} w^N_k + \int_v \frac{1}{f} \rho_2 \psi^N \ddot{u}^N_i \phi^M \, dv$$

$$+ \int_v \frac{1}{f^2} \rho_2 \phi^N \ddot{w}^N_i \phi^M \, dv + \int_v C_{ij} \phi^M \phi^N \dot{w}^N_j \, dv \qquad \text{(A-21)}$$

Define

$$\int_{S_3} \hat{\pi} n_j \Phi^M \, dS + \int_v \frac{1}{f} \rho_2 f_j \Phi^M \, dv = F^M_{fj}$$

$$\int_v M \alpha \psi^N_{,k} \Phi^M_{,j} \, dv = K^{NM}_{sfkj}$$

$$\int_v M \Phi^N_{,k} \Phi^M_{,j} \, dv = K^{NM}_{ffkj}$$

$$\int_v \frac{1}{f} \rho_2 \psi^N \Phi^M \, dv = M^{NM}_{sf} \qquad \text{(A-22)}$$

$$\int_v \frac{1}{f^2} \rho_2 \Phi^N \Phi^M \, dv = M^{NM}_{ff}$$

$$\int_v C_{jk} \Phi^N \Phi^M \, dv = C^{NM}_{ffjk}$$

Substituting Equation (A-22) into Equation (A-21)

$$F^M_{fj} = K^{NM}_{sfkj} \; u^N_k + K^{NM}_{ffkj} \; w^N_k + M^{NM}_{sf} \ddot{u}^N_j + M^{NM}_{ff} \ddot{w}^N_j + C^{NM}_{ffjk} \dot{w}^N_k \qquad \text{(A-23)}$$

Equations (A-20) and (A-23) can be written in matrix form as

$$\begin{bmatrix} K_{ss} & K_{sf} \\ K_{sf} & K_{ff} \end{bmatrix} \begin{Bmatrix} u \\ w \end{Bmatrix} + \begin{bmatrix} 0 & 0 \\ 0 & C_{ff} \end{bmatrix} \begin{Bmatrix} \dot{u} \\ \dot{w} \end{Bmatrix} + \begin{bmatrix} M_{ss} & M_{sf} \\ M_{sf} & M_{ff} \end{bmatrix} \begin{Bmatrix} \ddot{u} \\ \ddot{w} \end{Bmatrix} = \begin{Bmatrix} F_s \\ f_s \end{Bmatrix} \qquad \text{(A-24)}$$

END

FILMED

3-85

DTIC